



Quantifying the effects of solar geoengineering on vegetation

Katherine Dagon¹ · Daniel P. Schrag²

Received: 16 February 2018 / Accepted: 3 February 2019 / Published online: 09 February 2019
© Springer Nature B.V. 2019

Abstract

Climate change will have significant impacts on vegetation and biodiversity. Solar geoengineering has potential to reduce the climate effects of greenhouse gas emissions through albedo modification, yet more research is needed to better understand how these techniques might impact terrestrial ecosystems. Here, we utilize the fully coupled version of the Community Earth System Model to run transient solar geoengineering simulations designed to stabilize radiative forcing starting mid-century, relative to the Representative Concentration Pathway 6 (RCP6) scenario. Using results from 100-year simulations, we analyze model output through the lens of ecosystem-relevant metrics. We find that solar geoengineering improves the conservation outlook under climate change, but there are still potential impacts on terrestrial vegetation. We show that rates of warming and the climate velocity of temperature are minimized globally under solar geoengineering by the end of the century, while trends persist over land in the Northern Hemisphere. Moisture is an additional constraint on vegetation, and in the tropics the climate velocity of precipitation dominates over that of temperature. Shifts in the amplitude of temperature and precipitation seasonal cycles have implications for vegetation phenology. Different metrics for vegetation productivity also show decreases under solar geoengineering relative to RCP6, but could be related to the model parameterization of nutrient cycling. The coupling of water and carbon cycles is found to be an important mechanism for understanding changes in ecosystems under solar geoengineering.

Keywords Climate change · Solar geoengineering · Climate modeling · Terrestrial ecosystems

Electronic supplementary material The online version of this article (<https://doi.org/10.1007/s10584-019-02387-9>) contains supplementary material, which is available to authorized users.

Katherine Dagon
kdagon@ucar.edu

¹ National Center for Atmospheric Research, Boulder, CO, USA

² Department of Earth and Planetary Sciences, Harvard University, Cambridge, MA, USA

1 Introduction

Anthropogenic climate change is already having an impact on biodiversity and ecosystems. Recent studies have found evidence for species range shifts (Parmesan and Yohe 2003), alterations to phenology (Cleland et al. 2007), and changes in population dynamics (Bellard et al. 2012; Thuiller et al. 2008) due to biological impacts of climate change. Solar geoengineering is a proposed method of counteracting climate change through albedo modification to decrease incoming solar radiation (e.g., Crutzen 2006; Rasch et al. 2008; Shepherd and Rayner 2009; Keith and MacMartin 2015). Model simulations have found that decreasing incoming sunlight can help compensate for the climate effects of greenhouse gases such as carbon dioxide (CO_2) (Govindasamy and Caldeira 2000; Caldeira and Wood 2008; Kravitz et al. 2013). However, studies have also shown this compensation can lead to a decrease in regional precipitation (Bala et al. 2008; Schmidt et al. 2012; Kravitz et al. 2013; Niemeier et al. 2013; Tilmes et al. 2013; Kalidindi et al. 2015). The terrestrial hydrologic cycle is further influenced by changes in vegetation, for example, when changes in CO_2 influence stomatal conductance and other physiological factors affecting transpiration (Bala et al. 2006; Betts et al. 2007; Doutriaux-Boucher et al. 2009; Franks et al. 2013; Peng et al. 2014). Solar geoengineering is expected to have impacts on vegetation through both changes in the hydrologic cycle and feedbacks on plant physiology (Dagon and Schrag 2016).

Very little work has been focused on potential ecosystem impacts from solar geoengineering, despite the importance of understanding how these techniques might impact vegetation and biodiversity. Recent review papers have pointed to the need for more comprehensive assessments on how solar geoengineering of different forms might impact ecosystems (Russell et al. 2012; McCormack et al. 2016). One of the primary open questions is how vegetation might respond to a high- CO_2 , low temperature climate created by solar geoengineering, in contrast to the current low- CO_2 , low temperature climate, or the future high- CO_2 , high temperature climate with unmitigated global warming. A number of recent studies analyze the response of terrestrial productivity to solar geoengineering, but do not explicitly model shifts in vegetation distributions (Govindasamy et al. 2002; Naik et al. 2003; Jones et al. 2013; Glienke et al. 2015; Muri et al. 2015; Dagon and Schrag 2016; Xia et al. 2016; Ito 2017). Other studies have focused on the large-scale carbon cycle responses, including how changes in biogeochemical cycling impact precipitation (Fyfe et al. 2013) and how solar geoengineering impacts land and ocean carbon cycles (Tjiputra et al. 2016; Cao 2018). Typically, these studies use models that prescribe land surface vegetation distributions. While land surface schemes may dynamically evolve terrestrial carbon and nitrogen cycling including photosynthesis and leaf area index, the specific plant functional types remain fixed unless a dynamic ecosystem model is used (e.g., Fisher et al. 2015). Thus in order to simulate changes in biome boundaries in the absence of dynamic vegetation, ecosystem responses must be calculated from other climate model output such as temperature and precipitation. Climate classification systems have been used to study the effects of climate change on ecosystems and biodiversity (e.g., Leemans 1990; Fraedrich et al. 2001; Feng et al. 2012, 2014; Belda et al. 2016; Gallardo et al. 2016), but these systems have not yet been applied in the context of solar geoengineering. In addition, the climate velocity of temperature has been used to study the ability of species to adapt to climate changes (Loarie et al. 2009; Burrows et al. 2011; Burrows et al. 2014) and can be applied in a similar manner to model projections with solar geoengineering (Trisos et al. 2018).

In this paper, we analyze model output relevant to ecosystems, with the aim of understanding how geoengineering might impact adaptation and conservation efforts now and in the future. We explore changes in terrestrial vegetation under simulations of solar

geoengineering designed to stabilize global anthropogenic radiative forcing. In particular, we utilize a representation of solar geoengineering implementation that includes time-varying forcing. We first run a long-term transient climate simulation that is based on a policy-relevant climate change scenario. Two solar geoengineering simulations are designed to hold anthropogenic radiative forcing fixed at certain thresholds starting mid-century, relative to the climate change simulation. In our analysis, we study how the velocity of climate change, seasonality shifts, and productivity changes contribute to overall ecosystem responses and how these responses vary between model simulations with greenhouse warming and those simulations with solar geoengineering designed to stabilize anthropogenic radiative forcing by mid-century.

2 Methods

Here, we use the Community Earth System Model, version 1.2.2 (CESM1.2.2). We utilize a previously spun-up case to initialize our model simulations. Specifically, we choose a twentieth century transient all-forcing simulation run from 1850 to 2005. This run itself was initialized from a 1000-year pre-industrial control simulation (details on the available CESM experiments can be found at: <http://www.cesm.ucar.edu/experiments/cesm1.0>). These simulations were run fully coupled using physics from the Community Atmosphere Model, version 4 (CAM4), the Community Land Model, version 4 (CLM4), the Carbon-Nitrogen (CN) model for the land, and the full ocean model. The model horizontal resolution is 1.9° in latitude and 2.5° in longitude.

CLM4 is a dynamic land surface model developed by the National Center for Atmospheric Research (Oleson et al. 2010). The model separates grid cells into land surface type and simulates vertical moisture transport in a multilayer soil column model. Vegetated land units are further partitioned into at most 15 possible plant functional types (PFT) plus bare ground. Evaporative fluxes are a weighted averaged over all the PFT present in each land unit. Leaf and stem area indices as well as canopy top and bottom heights are determined dynamically using the fully prognostic CN model. The CN model simulates terrestrial biogeochemistry including phenology, vegetation structure, and carbon and nitrogen pools for leaves, stems, and roots. Dynamic vegetation is not active in this configuration of CLM, and as a result vegetation distributions are determined by satellite observations (Bonan et al. 2002). The model couples leaf stomatal conductance, needed for calculating transpiration, to leaf photosynthesis (Farquhar et al. 1980) and scales conductance with relative humidity and CO₂ concentration at the leaf surface (Collatz et al. 1991).

We first set up a control run using the Representative Concentration Pathway 6 (RCP6) forcing. This scenario, *RCP6*, is designed to hold radiative forcing fixed at 6 W m⁻² by the year 2100. We choose this scenario as a mid-range approximation of future emissions, a more conservative case than business-as-usual, but not as dramatic as some low-emissions scenarios (van Vuuren et al. 2011). The control run is set up identical to the aforementioned spin-up simulations, except with the forcing appropriate for the RCP6 future scenario (Masui et al. 2011; Fujino et al. 2006). This simulation is run for 50 years, from 2000 to 2050.

Results from RCP6 model year 2050 are used as starting conditions to branch off two solar geoengineering simulations. Accompanying the RCP6 forcing is a time-varying input for annual total solar irradiance (TSI), which is specified over the time period of 1610 to 2140 using the reconstruction from Lean et al. (1995). The first solar geoengineering simulation, *SG2050*, uses a modified TSI input file to hold the anthropogenic radiative forcing

fixed at year 2050 values as specified by RCP6. Specific values for RCP6 radiative forcing are calculated using the liveMAGICC model (Meinshausen et al. 2011), which can be accessed at: <http://live.magicc.org>. The solar modification is calculated by taking the known ratio of solar constant reduction to radiative forcing required to compensate a doubling of atmospheric CO₂ (Kravitz et al. 2015; Dagon and Schrag 2016) and multiplying it by the decrease in radiative forcing required for that year. We use the estimate of doubled CO₂ instantaneous radiative forcing of 3.7 W m⁻² from Myhre et al. (1998). The SG2050 simulation is then run for 50 years to finish at the beginning of year 2100.

The second solar geoengineering simulation, *SG2000*, again uses a modified TSI input file for a more aggressive geoengineering scenario. The solar forcing is designed to linearly ramp down radiative forcing from 2050 to 2000 values, as specified by RCP6, over the first 10 years. Then the radiative forcing is held fixed at year 2000 values. The same method for calculating solar reduction in the SG2050 simulation is used here. The model is again run for a total of 50 years to finish by the year 2100.

The RCP6 control is also run for an additional 50 years to finish at the same time as the solar geoengineering simulations. Figure S1 shows a schematic of the annual radiative forcing for all three simulations, and Fig. S2 details the annual solar reduction input for SG2050 and SG2000. All simulations are run at the same horizontal resolution as the spin-up, with monthly averaged atmosphere and land output files used in the analysis.

3 Results

The resulting global mean surface air temperature response for all three simulations is shown in Fig. 1. Our simulations behave as expected, with continuous warming in the RCP6 scenario and stabilized warming in the solar geoengineering runs. SG2050 keeps global temperature approximately constant around year 2050, while SG2000 ramps down the temperature to close to present-day values as reported by the model, though it overcompensates in some years.

We first utilize two climate classification systems to analyze changes in biome areas under solar geoengineering and climate change, based on model output of temperature and moisture-related variables. Both the simplified Köppen-Geiger and modified Thornthwaite systems show shifts in vegetation under solar geoengineering relative to RCP6, though we acknowledge the associated uncertainties with these systems (Supplemental Material, Tables S1-S3, Figs. S3-S5). To better investigate changes in vegetation, we focus on ecosystem-relevant model output such as the climate velocity, seasonality metrics, and coupled carbon-water fluxes.

3.1 Climate velocity

The rate of temperature change is important for species' abilities to adapt to changes in climate. In order to account for spatially varying changes in surface temperature, we analyze explicit rates of warming over time. Figure S6 shows warming per decade for 30-year periods. We use 30-year periods to avoid the strong cooling trend apparent in the first 10–20 years of the SG2000 simulation. This trend is due to its design to initially ramp down radiative forcing from 2050 back to 2000 levels. A warming signal is observed globally in the first and last 30 years of the 100-year RCP6 run. This trend is stronger at high latitudes. The trends in the SG2050 simulation are closer to zero, with some regional warming trends over land in the Northern Hemisphere and cooling in parts of the Southern Hemisphere. Cooling

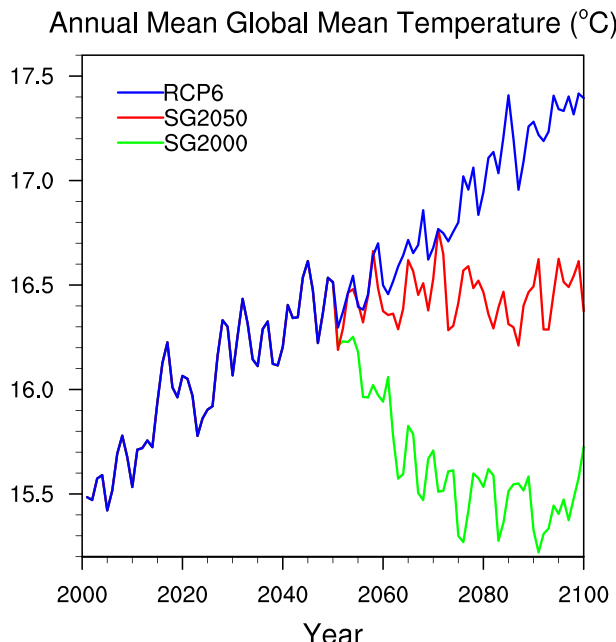


Fig. 1 Annual mean global mean surface air temperature for all three simulations

is observed across the tropics and Southern Hemisphere land area in SG2000, with residual warming in the Northern Hemisphere.

To test whether rates of warming have stabilized by the end of the century, we calculate land surface temperature trends over time globally and in both hemispheres using a moving 30-year window. The results for all three simulations are shown in Fig. S7. RCP6 shows a continuous positive trend in warming, with a larger rate in the Northern Hemisphere than in the Southern Hemisphere. Both solar geoengineering simulations approach zero global trends by 2100, with the SG2050 simulation stabilizing relatively quickly and the SG2000 simulation recovering from a cooling trend observed in the initial years of analysis. Both solar geoengineering simulations show warming trends in the Northern Hemisphere and cooling trends in the Southern Hemisphere by 2100.

To better connect with potential species range shifts, we also calculate the velocity of climate change as a measure of thermal shift (Loarie et al. 2009; Burrows et al. 2011, 2014). This measure represents the local surface velocity required to keep temperatures constant. The velocity of climate change is calculated as the 30-year decadal temperature trend (Fig. S6) divided by the spatial gradient of temperature (units of $^{\circ}\text{C km}^{-1}$) to result in units of km decade^{-1} . We use the average maximum technique to calculate a spatial gradient that combines changes in latitude and longitude (Loarie et al. 2009). The resulting climate velocities are shown in Fig. 2 for all four cases. The spatial responses are characteristically similar to what is observed in the rate of warming. However, the velocity of climate change shows a strong response in some areas, especially in the tropics. This is partially driven by the fact that the spatial gradient of temperature is small here, resulting in a larger climate velocity (Koven 2013). While the climate velocity increases throughout the RCP6 scenario, there is little observed increase over land in the SG2050 simulation, with some exceptions in the Northern Hemisphere. The SG2000 simulation shows a decrease in

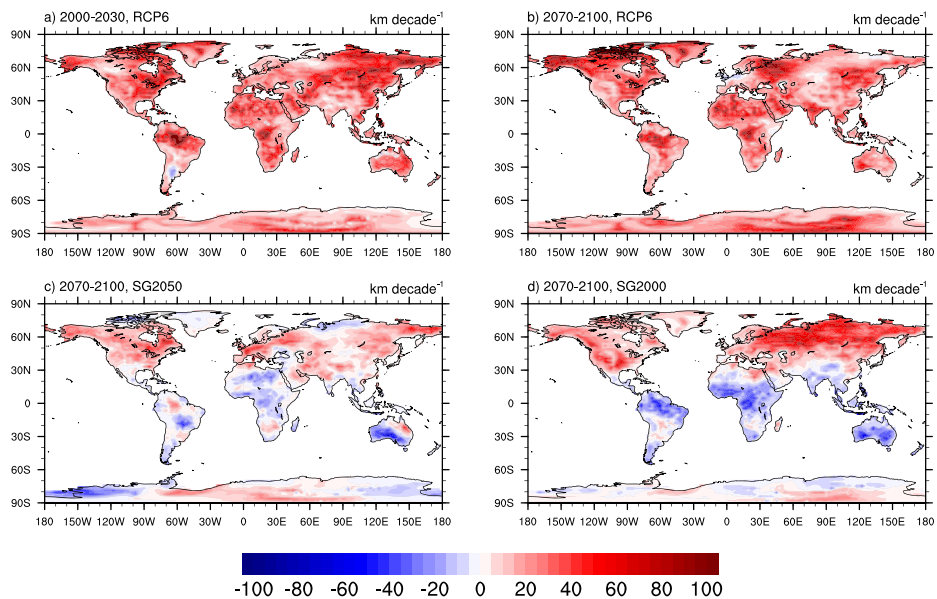


Fig. 2 The velocity of climate change (km decade^{-1}) derived from temperature changes for the first 30 years of RCP6 (a), the last 30 years of RCP6 (b), the last 30 years of SG2050 (c), and the last 30 years of SG2000 (d)

climate velocity in the tropics and Southern Hemisphere, and an increase in velocity in the Northern Hemisphere including areas in Russia and the central United States.

Moisture constraints are an important consideration for vegetation, and the climate velocity of temperature alone may not be sufficient to understand the potential responses of ecosystems to solar geoengineering. To address this, we also calculate the climate velocity of precipitation in a similar manner to that of temperature, by dividing the temporal change in monthly mean precipitation rate by the spatial gradient in precipitation. The results for all four time periods are shown in Fig. S8. These results do not show concise patterns or trends as seen in the temperature analysis, driven by the varying spatial responses of precipitation to both climate change and solar geoengineering. Because the sign of the climate velocity is driven by the temporal gradient, our results show increases and decreases in all scenarios; however, there are more decreases over land under solar geoengineering. To simplify these results and connect with the temperature analysis, we compare Fig. S8 with Fig. 2 and mask out regions where the climate velocity of temperature is greater than that of precipitation, since the two fields are both in units of km decade^{-1} . What is left is shown in Fig. S9, and highlights areas where precipitation changes dominate. There are not many regions evident under RCP6, but under solar geoengineering we see more land areas appear unmasked. Because temperature changes are minimized under solar geoengineering by design, the resulting precipitation changes become more important, even if they are relatively small.

3.2 Seasonality

Changes in seasonality can impart changes in phenology and thus affect the timing of vegetation life cycles. We analyze seasonal cycles of temperature and moisture to understand

how vegetation might be impacted by changes in seasonality. The top panels of Fig. 3 show global mean temperature and precipitation climatologies for 15-year periods. There is some implicit warming associated with the “present-day” climatology because we calculate it as the first 15 years of the RCP6 simulation; however, its effect is minimal. SG2000 slightly overcompensates but does the best job of returning the seasonal cycle of temperature to present day. However, SG2050 is the simulation that most closely matches the present-day climatology of global mean precipitation. SG2000 decreases precipitation in all months, relative to present day. Neither temperature nor precipitation show any major phase shift in the global mean climatology, and differences between the simulations are best characterized by shifts in amplitude.

To investigate how changes in climate from our simulations affect modeled changes in vegetation growth, we also plot changes in 15-year climatologies of net primary productivity (NPP) and leaf area index (LAI) relative to present day in the bottom panels of Fig. 3. Both solar geoengineering simulations show a large increase in NPP and LAI from present-day

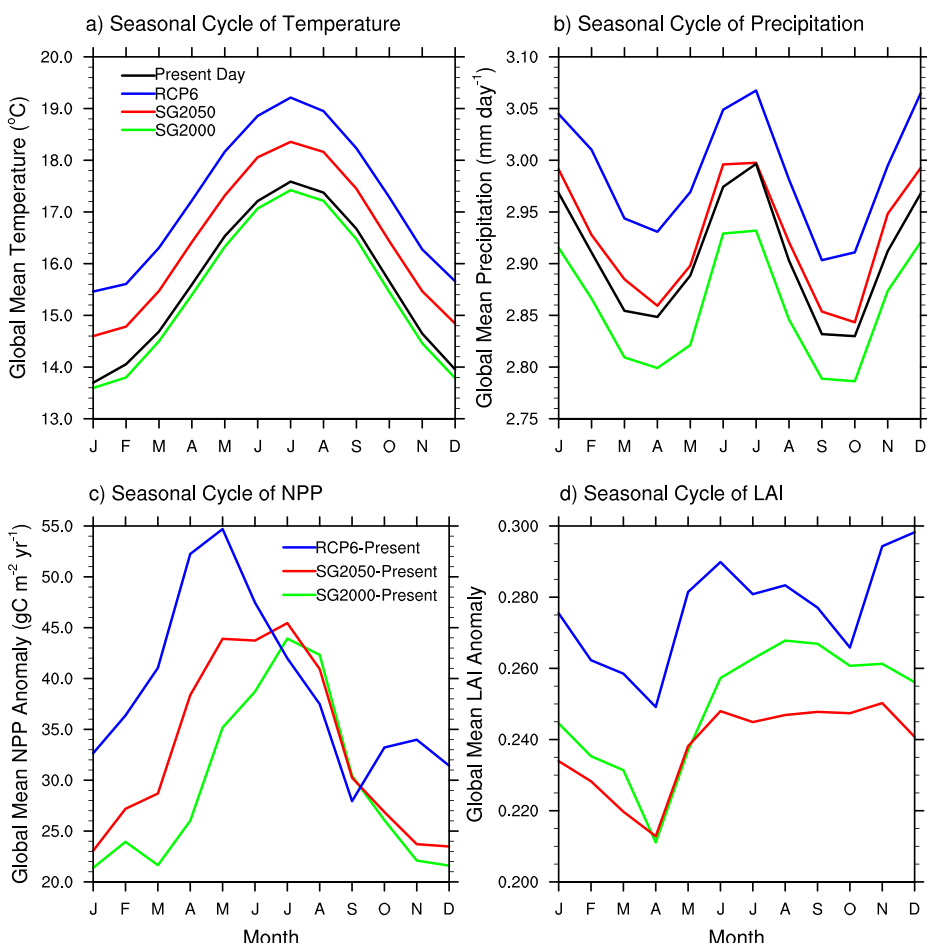


Fig. 3 15-year climatologies of global mean **a** temperature ($^{\circ}\text{C}$) and **b** precipitation (mm day^{-1}) for all four cases. Anomalies in 15-year climatologies of global mean **c** net primary productivity (NPP, $\text{gC m}^{-2} \text{ year}^{-1}$) and **d** leaf area index (LAI) for the three simulations, relative to present day

values due primarily to the increase in atmospheric CO₂. Relative to RCP6, solar geoengineering decreases NPP and LAI in most months except boreal summer when NPP increases on a global mean basis. While SG2000 has a greater effect on decreasing NPP relative to the climate change scenario than the effect of SG2050, the opposite is true for LAI. The response is fairly consistent across months, with again the exception of July–September for NPP and April–May for LAI.

3.3 Water and carbon fluxes

Water availability is a key element in the response of vegetation to climate changes. Previous studies have shown that solar geoengineering has regionally varying impacts on the terrestrial hydrologic cycle (Schmidt et al. 2012; Kravitz et al. 2013; Tilmes et al. 2013; Niemeier et al. 2013). In particular, water cycling slows down under model simulations of solar geoengineering, with less precipitation and less evapotranspiration over land (Dagon and Schrag 2016). These changes are driven both by the decrease in solar radiation and the increase of atmospheric CO₂. The former acts to limit surface energy available for evaporation, while the latter has a direct effect on plant physiology through stomatal conductance and photosynthesis.

Here, we more closely examine changes in water cycling under solar geoengineering relative to the RCP6 future scenario, as an additional constraint to quantifying terrestrial vegetation changes. Plots showing changes in 30-year mean precipitation minus evapotranspiration (P-ET) and soil moisture of the top 10 cm are shown in Fig. 4. By comparing solar

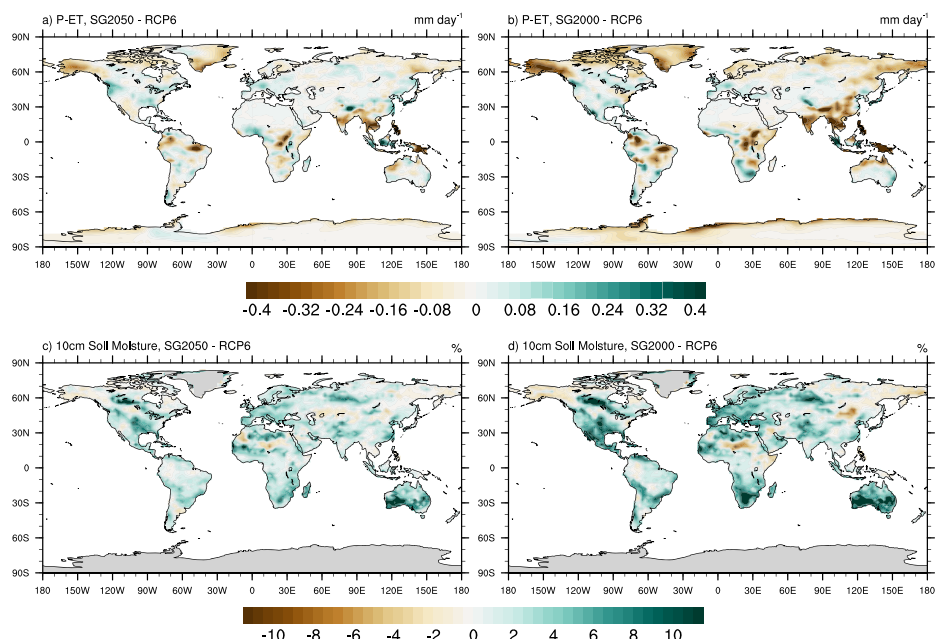


Fig. 4 Annual mean precipitation minus evapotranspiration (P-ET, mm/day) changes shown in panels (a) and (b), and soil moisture of the top 10 cm (%) changes shown in panels (c) and (d) for the last 30 years of the solar geoengineering simulations, relative to the last 30 years of RCP6. The left panels show SG2050 relative to RCP6, and the right panels show SG2000 relative to RCP6

geoengineering with RCP6, we focus on simulations that have the same CO₂ forcing over time and thus will not show the influence of CO₂ on changes in water cycling. However, these comparisons do highlight how changes in solar radiation affect surface hydrology. ET mostly decreases over land due to less energy input into the surface and less vegetation productivity, the latter of which limits plant water use. However, P-ET changes are largely driven by the precipitation response, which varies locally. There are large areas where soil moisture increases, though less so in places where P-ET decreases significantly.

In the top panels of Fig. 5, we show zonal mean changes in the three fluxes contributing to ET changes over land: ground evaporation, canopy evaporation, and plant transpiration. This analysis helps shed light on what mechanisms are driving changes in total ET. For both solar geoengineering simulations we see that transpiration is driving most of the large decreases in ET over land. Furthermore, there are specific latitude bands that have the largest decreases in transpiration and thus ET, namely around 40 °S (southern South America),

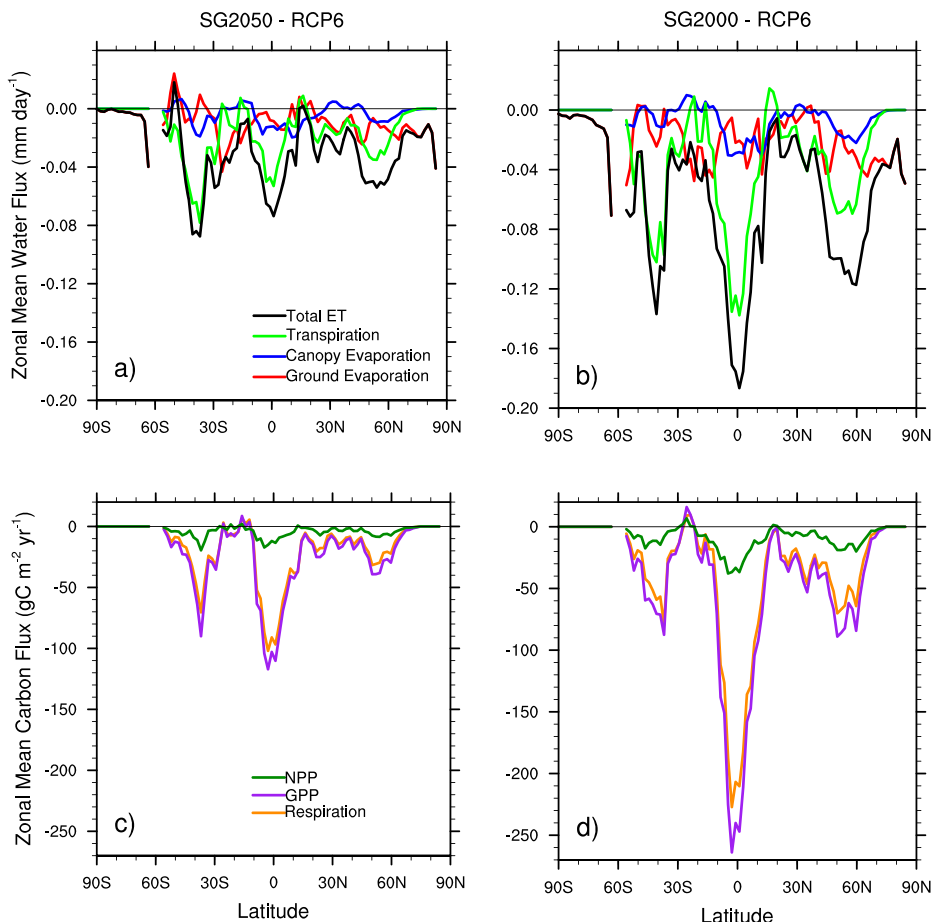


Fig. 5 Annual mean, zonal mean changes in land water fluxes (mm/day) shown in panels (a) and (b), and land carbon fluxes ($\text{gC m}^{-2} \text{year}^{-1}$) shown in panels (c) and (d) for the last 30 years of the solar geoengineering simulations, relative to the last 30 years of RCP6. The left panels show SG2050 relative to RCP6, and the right panels show SG2000 relative to RCP6

the equator (Amazon, Congo, and southeast Asia), and 50 °N (eastern North America and parts of Russia). Changes in ground and canopy evaporation are small by comparison, but both show decreases over almost all latitudes. In general, changes are larger in the SG2000 simulation than in SG2050, due to the greater decrease in solar radiation when comparing that simulation with RCP6. We further see that the decreases in zonal mean transpiration are matched by decreases in land carbon fluxes (bottom panels of Fig. 5), demonstrating that the coupling between vegetation water use and productivity is driving the response of ET over land. While gross primary productivity (GPP) and respiration decreases are of similar magnitude, GPP changes dominate at almost all latitudes driving an overall decrease in NPP.

4 Discussion

Ecosystems will be impacted by climate change in a multitude of ways. Here, we contrast the response of terrestrial vegetation under a model simulation with greenhouse warming to simulations with solar geoengineering. To target ecosystem impacts, we focus on temporal and spatial trends in temperature, hydrology, and plant growth. Overall, our results show that solar geoengineering produces a twenty-first century climate that is more favorable for vegetation than the simulation with greenhouse warming. However, there are still changes that occur under solar geoengineering that could have implications for future conservation and biodiversity.

To explore changes in vegetation, we first analyze global rates of surface temperature change. Thirty-year time periods show robust warming trends in RCP6, little change in SG2050, and cooling in SG2000 with the exception of Northern Hemisphere high latitudes where there is a residual warming trend (Fig. S6). The trends for all scenarios are generally stronger in the Northern Hemisphere than in the Southern Hemisphere (Fig. S7). Given that warming is implied for the first 50 years of our RCP6 simulation, the benefit to a delayed solar geoengineering implementation will be limited to species that can adapt to initial climate changes. A stabilized or cooled climate after 2050 will help prevent further vegetation shifts or extinctions, with the exception of species that have already adapted to a higher mean temperature and may not survive if the climate is cooled back down. The time history of temperature change is crucial in an ecosystems context (Parmesan and Yohe 2003; Loarie et al. 2009; Higgins and Scheiter 2012); while some species may persist through initial warming, others may disappear before the climate can be cooled in the second half of the century. Furthermore, warming trends persist in the Northern Hemisphere, suggesting ecosystems in those places will still have to adapt to increases in temperature by the end of the century even with solar geoengineering as we have specified it here. The residual warming in the Northern Hemisphere echoes results shown in other studies where uniform solar geoengineering creates a meridional gradient in boreal summer surface temperature (Dagon and Schrag 2017). High latitudes warm more than low latitudes, due to the seasonal and spatial pattern of solar radiation (Kravitz et al. 2013).

Changes in climate velocity help map potential geographic shifts over time. Increases in the climate velocity of temperature observed over land in the RCP6 simulation are compensated for in the solar geoengineering simulations, with potential benefits for terrestrial species that might otherwise be limited in their ability to adapt to thermal shifts (Fig. 2). Areas of slow velocity could act as repositories for biodiversity if other regions are threatened (Burrows et al. 2011). While plants will certainly respond to aspects of climate other than just temperature, the climate velocity calculated here gives a first order assessment of how the thermal environment might impact vegetation. Moisture constraints are an

important consideration, yet calculation of the climate velocity of precipitation did not show clear trends (Fig. S8). However, when the climate velocity magnitudes were compared across temperature and precipitation, regions in the tropics emerged as having a greater climate velocity of precipitation under solar geoengineering, despite reduced thermal risks (Fig. S9). This result indicates greater sensitivity of tropical ecosystems to future hydrologic changes under uniform solar geoengineering. It is important to note that species may not move at constant rates, for example an uphill movement may proceed at a different rate than a downhill migration (Loarie et al. 2009), and thus, the velocities presented here are relative to climate changes, not indicators of precise migration rates.

Changes in seasonality on a global mean basis show that SG2000 is better suited to compensate large-scale climatological changes in temperature from RCP6, while SG2050 is more appropriate for precipitation changes (Fig. 3a and b). This point illustrates the difficulty that model simulations of solar geoengineering have in simultaneously compensating for temperature and precipitation changes from global warming (e.g., Ricke et al. 2010). While these results do not show major shifts in the phase of temperature or precipitation annual cycles, a change in amplitude alone can cause phenological impacts such as earlier flowering or leafing (Cleland et al. 2007; Wolkovich et al. 2012). NPP and LAI show global mean seasonality decreases under solar geoengineering relative to RCP6, fairly consistently throughout the annual cycle (Fig. 3c and d). The global mean NPP response seems to be driven mostly by mid-latitude regions such as the Central US and western Europe, though the Amazon response shows similar characteristics (Fig. S10). LAI also shows regionally varying climatological responses, with some regions showing an increase in leaf area under one solar geoengineering simulation and a decrease in the other (Fig. S11). This implies that a variety of mechanisms could be responsible for the productivity responses, such that NPP responds to different climate drivers than what LAI is most sensitive to Luo et al. (2004). While the land surface model used here does include active carbon cycling and plant growth, the specific plant functional types are fixed by satellite data (Bonan et al. 2002). The model may evolve NPP and LAI in response to climate changes, but the vegetation composition does not respond dynamically. This limitation illustrates why we also explore climate classifications of vegetation using the climate envelope approach, as a substitute for explicitly modeling plant types (Supplemental Material). It is expected that phenology will shift with climate change (Walther et al. 2002; Parmesan and Yohe 2003; Burrows et al. 2011), and further investigating how solar geoengineering might compensate seasonal shifts in vegetation is an important topic for future work.

Changes in water cycling are essential to understanding vegetation impacts under solar geoengineering. Our simulations show areas of P-ET increase and decrease over land, under solar geoengineering relative to RCP6 (Fig. 4a and b). Despite regional heterogeneity in P-ET, soil moisture increases over most of the land area (Fig. 4c and d), indicating that terrestrial water storage could increase under solar geoengineering. A closer examination of changes in land water fluxes shows that transpiration is driving most of the ET decreases over land, with certain latitude bands (including the tropics) affected more than others (Fig. 5a and b). Decreasing plant water use due to a decrease in transpiration is likely driving the increase in global soil moisture. Changes in water cycling in tropical rainforests will certainly have downstream impacts on biodiversity (Myers et al. 2000; Lewis et al. 2004). Furthermore zonal mean changes in land carbon fluxes match the pattern of decreases in transpiration (Fig. 5c and d), suggesting that it is the inherent plant response driving the terrestrial hydrologic response to solar geoengineering, rather than surface energy limitation. The direct response of less sunlight could decrease NPP, though modeling studies with

solar geoengineering of a similar magnitude have demonstrated that this effect is small (Govindasamy et al. 2002; Naik et al. 2003).

Here, we prescribe solar geoengineering as a decrease in solar radiation, an approximation for stratospheric aerosol injection. As a result, we do not include potential changes in the partitioning of diffuse and direct radiation. Aerosols tend to scatter incoming radiation, resulting in a greater diffuse fraction. Enhancements in the diffuse fraction have been shown in observations and modeling studies to increase vegetation productivity, because plants are able to more efficiently utilize the incoming radiation without becoming light-saturated (Gu et al. 2002; Mercado et al. 2003; Alton et al. 2007; Cheng et al. 2015). This response varies regionally and depends on canopy structure, and in some cases, the increased diffuse fraction may not compensate for the overall decrease in available light (Tingley et al. 2014; Kalidindi et al. 2015; Proctor et al. 2018). Xia et al. (2016) included changes in diffuse radiation under model simulations of solar geoengineering, and found that globally averaged photosynthesis increased relative to RCP6. This effect was due to both the diffuse enhancement as well as the cooling effect of solar geoengineering, with the global response driven primarily by the increase in productivity in the tropics. High latitudes showed an overall decrease in photosynthesis because the temperature effect dominated over the radiation effect (Xia et al. 2016). However, this study did not use the CN model with CLM, and thus the photosynthesis response does not include potential changes in LAI and nutrient cycling, important potential feedbacks shown in our results. Because our simulations do not include the diffuse enhancement, our results are more indicative of the effect of changes in temperature, hydrology, and biogeochemistry on plant productivity rather than radiation impacts or changes in plant types and distributions.

A potential source of uncertainty in our results is the use of a single climate model to study the vegetation responses to solar geoengineering. Previous studies using model intercomparisons have shown a wide range of NPP responses to solar geoengineering (Jones et al. 2013; Gienke et al. 2015). One of the primary reasons for this difference is whether or not the land model includes an active nitrogen cycle (Cao 2018). Other studies have pointed to the importance of the nitrogen cycle in CLM4 (Bonan and Levis 2010; Irvine et al. 2014; Lee et al. 2013). Models with nitrogen cycling show an increase in soil respiration with warming, which increases nitrogen availability and NPP where nitrogen is limiting. On the other hand, models without nitrogen cycling could overestimate the CO₂ fertilization effect because they do not account for nutrient limitation (Thornton et al. 2007). Our results show a global decrease in NPP under solar geoengineering relative to RCP6, because surface cooling and nitrogen cycling limit nutrient availability, and there is no CO₂ fertilization to compensate the loss of productivity. This result is consistent with the sign of the global mean NPP responses of Gienke et al. (2015) when considering the models that include a nitrogen cycle. While nitrogen cycling does act to decrease respiration influenced by the cooling effect of solar geoengineering, we find that the zonal mean NPP decrease is driven by a decrease in GPP which dominates over the decrease in respiration. However, if these decreases in NPP and ET are exaggerated by the model, the increase in soil moisture under solar geoengineering could be overestimated.

Finally, there is uncertainty in ecological impacts as related to the implementation of solar geoengineering and the choice of emissions scenario. It is challenging to predict the impacts of solar geoengineering on vegetation when those impacts are sensitive to the choice of scenario. Previous studies have shown that the climate response to geoengineering may be roughly linear in terms of global mean temperature, but regional and seasonal changes and hydrologic responses exhibit nonlinearities (Dagon and Schrag 2016; Irvine et al. 2010; Modak and Bala 2014; Kravitz et al. 2014). The termination effect is also discussed in this

context, as in the possible shock to the climate system that would occur if solar geoengineering were imposed and then suddenly discontinued (Jones et al. 2013; McCusker et al. 2014; Ito 2017; Trisos et al. 2018). Here, we model solar geoengineering in a transient manner, to stabilize global radiative forcing as greenhouse gases continue to increase during the second half of the twenty-first century. Our results are very much dependent on the choice of geoengineering and emissions scenarios, and how the resulting climate changes influence vegetation. In the future it will be important to consider a range of models and scenarios to capture the full spread of ecosystems responses to solar geoengineering.

5 Conclusions

We have demonstrated potential impacts on terrestrial ecosystems due to solar geoengineering simulations that minimize anthropogenic radiative forcing by mid-century. Rates of warming and the climate velocity associated with temperature changes are both minimized under solar geoengineering relative to the greenhouse gas forcing simulation. However, warming trends persist over land in the Northern Hemisphere, and the delayed implementation of solar geoengineering assumes ecosystems survive long enough to see the potential benefits. Global mean seasonal cycles of vegetation-related climate variables show shifts in amplitude but not phase, and have implications for plant phenology. Modeled productivity metrics show varying responses to solar geoengineering, but could be affected by land surface model biases. Changes in water cycling confirm that the vegetation response to solar geoengineering is driving the response of terrestrial hydrology, though these changes are inherently tied to the model representations of carbon, nitrogen, and water.

Both solar geoengineering simulations generate a climate that is better suited for preserving vegetation than the changes induced by greenhouse warming. Nevertheless, there are still changes in climate under solar geoengineering that would impact future ecosystems. Regional rates of warming remain elevated in the Northern Hemisphere and seasonal shifts are likely due to changes in productivity. While terrestrial water storage may increase through a decrease in evapotranspiration, changes in vegetation water cycling, especially in tropical regions, are likely to impact biodiversity. Arguments that solar geoengineering can effectively neutralize all vegetation shifts are not straightforward. Instead our model results indicate a nuanced situation and highlight important tradeoffs. Though solar geoengineering might make certain aspects of conservation easier, strategies for biodiversity and habitat preservation will need to adapt to suit the resulting climate changes.

Acknowledgements We thank the editor and two anonymous reviewers for suggestions that improved the paper. The model simulations in this paper were run on the Odyssey cluster supported by the FAS Division of Science, Research Computing Group at Harvard University. We thank Zhiming Kuang for the use of his computational resources. Further data analysis was completed using the computing resources of the Climate and Global Dynamics Information Systems Group at the National Center for Atmospheric Research. The National Center for Atmospheric Research is sponsored by the National Science Foundation.

Funding information This received funding from the NCAR Advanced Study Program.

Publisher's note Springer Nature remains neutral with regard to jurisdictional claims in published maps and institutional affiliations.

References

- Alton PB, North PR, Los SO (2007) The impact of diffuse sunlight on canopy light-use efficiency, gross photosynthetic product and net ecosystem exchange in three forest biomes. *Glob Chang Biol* 13:776–787
- Bala G, Caldeira K, Mirin A, Wickett M, Delire C, Phillips TJ (2006) Biogeophysical effects of CO₂ fertilization on global climate. *Tellus B Chem Phys Meteorol* 58(5):620–627
- Bala G, Duffy PB, Taylor KE (2008) Impact of geoengineering schemes on the global hydrological cycle. *Proc Natl Acad Sci* 105(22):7664–7669
- Belda M, Holtanová E, Kalvová J, Halenka T (2016) Global warming-induced changes in climate zones based on CMIP5 projections. *Clim Res* 71(1):17–31
- Bellard C, Bertelsmeier C, Leadley P, Thuiller W, Courchamp F (2012) Impacts of climate change on the future of biodiversity. *Ecol Lett* 15(4):365–377
- Betts RA, Boucher O, Collins M, Cox PM, Falloon PD, Gedney N, Hemmin DL, Huntingford C, Jones CD, Sexton DM, Webb MJ (2007) Projected increase in continental runoff due to plant responses to increasing carbon dioxide. *Nature* 448(7157):1037–1041
- Bonan GB, Levis S (2010) Quantifying carbon-nitrogen feedbacks in the Community Land Model (CLM4). *Geophys Res Lett* 37(7):L07401
- Bonan GB, Levis S, Kergoat L, Oleson KW (2002) Landscapes as patches of plant functional types: an integrating concept for climate and ecosystem models. *Glob Biogeochem Cycles* 16(2). <https://doi.org/10.1029/2000GB001360>
- Burrows MT, Schoeman DS, Buckley LB, Moore P, Poloczanska ES, Brander KM, Brown C, Bruno JF, Duarte CM, Halpern BS, Holding J, Kappel CV, Kiessling W, O'Connor MI, Pandolfi JM, Parmesan C, Schwing FB, Sydeman WJ, Richardson AJ (2011) The pace of shifting climate in marine and terrestrial ecosystems. *Science* 334(6056):652–655
- Burrows MT, Schoeman DS, Richardson AJ, Molinos JG, Hoffmann A, Buckley LB, Moore PJ, Brown CJ, Bruno JF, Duarte CM, Halpern BS, Hoegh-Guldberg O, Kappel CV, Kiessling W, O'Connor MI, Pandolfi JM, Parmesan C, Sydeman WJ, Ferrier S, Williams KJ, Poloczanska ES (2014) Geographical limits to species-range shifts are suggested by climate velocity. *Nature* 507(7493):492–495
- Caldeira K, Wood L (2008) Global and Arctic climate engineering: numerical model studies. *Philosophical Transactions of the Royal Society A: Mathematical, Phys Eng Sci* 366(1882):4039–4056
- Cao L (2018) The effects of solar radiation management on the carbon cycle. *Current Climate Change Reports* 4(1):41–50
- Cheng SJ, Bohrer G, Steiner AL, Hollinger DY, Suyker A, Phillips RP, Nadelhoffer KJ (2015) Variations in the influence of diffuse light on gross primary productivity in temperate ecosystems. *Agric For Meteorol* 201:98–110
- Cleland EE, Chuine I, Menzel A, Mooney HA, Schwartz MD (2007) Shifting plant phenology in response to global change. *Trends Ecol Evol* 22(7):357–365
- Collatz GJ, Ball JT, Grivet C, Berry JA (1991) Physiological and environmental regulation of stomatal conductance, photosynthesis and transpiration: a model that includes a laminar boundary layer. *Agric For Meteorol* 54:107–136
- Crutzen PJ (2006) Albedo enhancement by stratospheric sulfur injections: a contribution to resolve a policy dilemma? *Clim Chang* 77:211–220
- Dagon K, Schrag DP (2016) Exploring the effects of solar radiation management on water cycling in a coupled land-atmosphere model. *J Clim* 29(7):2635–2650
- Dagon K, Schrag DP (2017) Regional climate variability under model simulations of solar geoengineering. *J Geophys Res: Atmos* 122(22):12,106–12,121. 2017JD027110
- Doutriaux-Boucher M, Webb MJ, Gregory JM, Boucher O (2009) Carbon dioxide induced stomatal closure increases radiative forcing via a rapid reduction in low cloud. *Geophys Res Lett* 36(2):L02703
- Farquhar GD, von Caemmerer S, Berry JA (1980) A biochemical model of photosynthetic CO₂ assimilation in leaves of C₃ species. *Planta* 149:78–90
- Feng S, Ho C-H, Hu Q, Oglesby RJ, Jeong S-J, Kim B-M (2012) Evaluating observed and projected future climate changes for the Arctic using the köppen-Trewartha climate classification. *Clim Dyn* 38(7):1359–1373
- Feng S, Hu Q, Huang W, Ho C-H, Li R, Tang Z (2014) Projected climate regime shift under future global warming from multi-model, multi-scenario CMIP5 simulations. *Glob Planet Chang* 112:41–52
- Fisher RA, Muszala S, Verteinstein M, Lawrence P, Xu C, McDowell NG, Knox RG, Koven C, Holm J, Rogers BM, Spessa A, Lawrence D, Bonan G (2015) Taking off the training wheels: the properties of

- a dynamic vegetation model without climate envelopes, CLM4.5(ED). *Geosci Model Dev* 8(11):3593–3619
- Fraedrich K, Gerstengarbe F-W, Werner PC (2001) Climate shifts during the last century. *Clim Chang* 50(4):405–417
- Franks PJ, Adams MA, Amthor JS, Barbour MM, Berry JA, Ellsworth DS, Farquhar GD, Ghannoum O, Lloyd J, McDowell N, Norby RJ, Tissue DT, von Caemmerer S (2013) Sensitivity of plants to changing atmospheric CO₂ concentration: from the geological past to the next century. *New Phytol* 197(4):1077–1094
- Fujino J, Nair R, Kainuma M, Masui T, Matsuoka Y (2006) Multi-gas mitigation analysis on stabilization scenarios using aim global model. *Energy J* 27:343–353
- Fyfe JC, Cole JNS, Arora VK, Scinocca JF (2013) Biogeochemical carbon coupling influences global precipitation in geoengineering experiments. *Geophys Res Lett* 40(3):651–655
- Gallardo C, Gil V, Tejeda C, Sánchez E, Gaertner MA (2016) Köppen-trewartha classification used to assess climate changes simulated by a regional climate model ensemble over South America. *Clim Res* 68(2–3):137–149
- Glienke S, Irvine PJ, Lawrence MG (2015) The impact of geoengineering on vegetation in experiment G1 of the geoMIP. *J Geophys Res: Atmos* 120(19):10196–10213
- Govindasamy B, Caldeira K (2000) Geoengineering Earth's radiation balance to mitigate CO₂-induced climate change. *Geophys Res Lett* 27(14):2141–2144
- Govindasamy B, Thompson S, Duffy PB, Caldeira K, Delire C (2002) Impact of geoengineering schemes on the terrestrial biosphere. *Geophys Res Lett* 29(22):2061. <https://doi.org/10.1029/2002GL015911>
- Gu L, Baldocchi D, Verma SB, Black TA, Vesala T, Falge EM, Dowty PR (2002) Advantages of diffuse radiation for terrestrial ecosystem productivity. *J Geophys Res* 107(D6). <https://doi.org/10.1029/2001JD001242>
- Higgins SI, Scheiter S (2012) Atmospheric CO₂ forces abrupt vegetation shifts locally, but not globally. *Nature* 488(7410):209–212
- Irvine PJ, Ridgwell A, Lunt DJ (2010) Assessing the regional disparities in geoengineering impacts. *Geophys Res Lett* 37:L18702. <https://doi.org/10.1029/2010GL044447>
- Irvine PJ, Boucher O, Kravitz B, Alterskjær K, Cole JNS, Ji D, Jones A, Lunt DJ, Moore JC, Muri H, Niemeier U, Robock A, Singh B, Tilmes S, Watanabe S, Yang S, Yoon J-H (2014) Key factors governing uncertainty in the response to sunshade geoengineering from a comparison of the GeoMIP ensemble and a perturbed parameter ensemble. *J Geophys Res: Atmos* 119(13):7946–7962
- Ito A (2017) Solar radiation management and ecosystem functional responses. *Clim Chang* 142(1):53–66
- Jones A, Haywood JM, Alterskjær K, Boucher O, Cole JNS, Curry CL, Irvine PJ, Ji D, Kravitz B, Kristjánsson JE, Moore JC, Niemeier U, Robock A, Schmidt H, Singh B, Tilmes S, Watanabe S, Yoon J-H (2013) The impact of abrupt suspension of solar radiation management (termination effect) in experiment G2 of the Geoengineering Model Intercomparison Project (GeoMIP). *J Geophys Res: Atmos* 118(17):9743–9752
- Kalidindi S, Bala G, Modak A, Caldeira K (2015) Modeling of solar radiation management: a comparison of simulations using reduced solar constant and stratospheric sulphate aerosols. *Clim Dyn* 44(9):2909–2925
- Keith DW, MacMartin DG (2015) A temporary, moderate and responsive scenario for solar geoengineering. *Nat Clim Chang* 5(3):201–206
- Koven CD (2013) Boreal carbon loss due to poleward shift in low-carbon ecosystems. *Nat Geosci* 6:452–456
- Kravitz B, Caldeira K, Boucher O, Robock A, Rasch PJ, Alterskjær K, Karam DB, Cole JNS, Curry CL, Haywood JM, Irvine PJ, Ji D, Jones A, Kristjánsson JE, Lunt DJ, Moore JC, Niemeier U, Schmidt H, Schulz M, Singh B, Tilmes S, Watanabe S, Yang S, Yoon J-H (2013) Climate model response from the Geoengineering Model Intercomparison Project (GeoMIP). *J Geophys Res* 118(15):1–13
- Kravitz B, Rasch PJ, Forster PM, Andrews T, Cole JNS, Irvine PJ, Ji D, Kristjánsson JE, Moore JC, Muri H, Niemeier U, Robock A, Singh B, Tilmes S, Watanabe S, Yoon J-H (2013) An energetic perspective on hydrological cycle changes in the Geoengineering Model Intercomparison Project. *J Geophys Res: Atmos* 118 (23):13087–13102
- Kravitz B, MacMartin DG, Robock A, Rasch PJ, Ricke KL, Cole JNS, Curry CL, Irvine PJ, Ji D, Keith DW, Kristjansson JE, Moore JC, Muri H, Singh B, Tilmes S, Watanabe S, Yang S, Yoon J-H (2014) A multi-model assessment of regional climate disparities caused by solar geoengineering. *Environ Res Lett* 9(7):074013. <https://doi.org/10.1088/1748-9326/9/7/074013>
- Kravitz B, MacMartin DG, Rasch PJ, Jarvis AJ (2015) A new method of comparing forcing agents in climate models. *J Clim* 28(20):8203–8218
- Lean J, Beer J, Bradley R (1995) Reconstruction of solar irradiance since 1610: Implications for climate change. *Geophys Res Lett* 22(23):3195–3198

- Lee E, Felzer BS, Kothavala Z (2013) Effects of nitrogen limitation on hydrological processes in CLM4-CN. *J Adv Model Earth Syst* 5(4):741–754
- Leemans R (1990) Possible changes in natural vegetation patterns due to global warming. IIASA Working Paper WP-90-008 International Institute for Applied Systems Analysis Laxenburg, Austria
- Lewis SL, Malhi Y, Phillips OL (2004) Fingerprinting the impacts of global change on tropical forests. *Philosophical Transactions of the Royal Society of London B: Biological Sciences* 359(1443):437–462
- Loarie SR, Duffy PB, Hamilton H, Asner GP, Field CB, Ackerly DD (2009) The velocity of climate change. *Nature* 462(7276):1052–1055
- Luo T, Pan Y, Ouyang H, Shi P, Luo J, Yu Z, Lu Q (2004) Leaf area index and net primary productivity along subtropical to alpine gradients in the Tibetan Plateau. *Glob Ecol Biogeogr* 13(4):345–358
- Masui T, Matsumoto K, Hijioka Y, Kinoshita T, Nozawa T, Ishiwatari S, Kato E, Shukla PR, Yamagata Y, Kainuma M (2011) An emission pathway for stabilization at 6 W m^{-2} radiative forcing. *Clim Chang* 109(1):59
- McCormack CG, Born W, Irvine PJ, Achterberg EP, Amano T, Ardrion J, Foster PN, Gattuso J-P, Hawkins SJ, Hendy E, Kissling WD, Lluch-Cota SE, Murphy EJ, Ostle N, Owens NJP, Perry RI, Pörtner HO, Scholes RJ, Schurr FM, Schweiger O, Settele J, Smith RK, Smith S, Thompson J, Tittensor DP, van Kleunen M, Vivian C, Vohland K, Warren R, Watkinson AR, Widdicombe S, Williamson P, Woods E, Blackstock JJ, Sutherland WJ (2016) Key impacts of climate engineering on biodiversity and ecosystems, with priorities for future research. *J Integr Environ Sci* 13(2-4):103–128
- McCusker KE, Armour KC, Bitz CM, Battisti DS (2014) Rapid and extensive warming following cessation of solar radiation management. *Environ Res Lett* 9 (2):024005
- Meinshausen M, Raper SCB, Wigley TML (2011) Emulating coupled atmosphere-ocean and carbon cycle models with a simpler model, MAGICC6 – Part 1: model description and calibration. *Atmos Chem Phys* 11(4):1417–1456
- Mercado LM, Bellouin N, Sitch S, Boucher O, Huntingford C, Wild M, Cox PM (2003) Impact of changes in diffuse radiation on the global land carbon sink. *Nature* 458:1014–1017
- Modak A, Bala G (2014) Sensitivity of simulated climate to latitudinal distribution of solar insolation reduction in solar radiation management. *Atmos Chem Phys* 14(15):7769–7779
- Muri H, Niemeier U, Kristjánsson JE (2015) Tropical rainforest response to marine sky brightening climate engineering. *Geophys Res Lett* 42(8):2951–2960
- Myers N, Mittermeier RA, Mittermeier CG, da Fonseca GAB, Kent J (2000) Biodiversity hotspots for conservation priorities. *Nature* 403:853–858
- Myhre G, Highwood EJ, Shine KP, Stordal F (1998) New estimates of radiative forcing due to well mixed greenhouse gases. *Geophys Res Lett* 25(14):2715–2718
- Naik V, Wuebbles DJ, Delucia EH, Foley JA (2003) Influence of geoengineered climate on the terrestrial biosphere. *Environ Manag* 32(3):373–381
- Niemeier U, Schmidt H, Alterskjær K, Kristjánsson JE (2013) Solar irradiance reduction via climate engineering: Impact of different techniques on the energy balance and the hydrological cycle. *J Geophys Res* 118(21):11905–11917
- Oleson KW, Lawrence DM, Bonan GB, Flanner MG, Kluzek E, Lawrence PJ, Levis S, Swenson SC, Thornton PE (2010) Technical Description of version 4.0 of the Community Land Model (CLM). Technical Report TN-478+STR National Center for Atmospheric Research
- Parmesan C, Yohe G (2003) A globally coherent fingerprint of climate change impacts across natural systems. *Nature* 421(6918):37–42
- Peng J, Dan L, Dong W (2014) Are there interactive effects of physiological and radiative forcing produced by increased CO_2 concentration on changes of land hydrological cycle? *Glob Planet Chang* 112:64–78
- Proctor J, Hsiang S, Burney J, Burke M, Schlenker W (2018) Estimating global agricultural effects of geoengineering using volcanic eruptions. *Nature* 560(7719):480–483
- Rasch PJ, Crutzen PJ, Coleman DB (2008) Exploring the geoengineering of climate using stratospheric sulfate aerosols: the role of particle size. *Geophys Res Lett* 35:L02809. <https://doi.org/10.1029/2007GL032179>
- Ricke KL, Morgan MG, Allen MR (2010) Regional climate response to solar-radiation management. *Nat Geosci* 3(8):537–541
- Russell LM, Rasch PJ, Mace GM, Jackson RB, Shepherd J, Liss P, Leinen M, Schimel D, Vaughan NE, Janetos AC, Boyd PW, Norby RJ, Caldeira K, Merikanto J, Artaxo P, Melillo J, Morgan MG (2012) Ecosystem impacts of geoengineering: a review for developing a science plan. *AMBIO* 41(4):350–369
- Schmidt H, Alterskjær K, Karam DB, Boucher O, Jones A, Kristjánsson JE, Niemeier U, Schulz M, Aaheim A, Benduhn F, Lawrence M, Timmreck C (2012) Solar irradiance reduction to counteract radiative forcing from a quadrupling of CO_2 : Climate responses simulated by four earth system models. *Earth Syst Dynam* 3(1):63–78

- Shepherd J, Rayner S (2009) Geoengineering the climate: science, governance and uncertainty. Policy Doc. 10/09 RS1636 The Royal Society
- Thornton PE, Lamarque J-F, Rosenbloom NA, Mahowald NM (2007) Influence of carbon-nitrogen cycle coupling on land model response to CO₂ fertilization and climate variability. *Global Biogeochem Cycles* 21:GB4018. <https://doi.org/10.1029/2006GB002868>
- Thuiller W, Albert C, Araújo MB, Berry PM, Cabeza M, Guisan A, Hickler T, Midgley GF, Paterson J, Schurr FM, Sykes MT, Zimmermann NE (2008) Predicting global change impacts on plant species' distributions: future challenges. *Perspectives in Plant Ecology, Evolution and Systematics* 9(3):137–152. Space matters - Novel developments in plant ecology through spatial modelling
- Tilmes S, Fasullo J, Lamarque J-F, Marsh DR, Mills M, Alterskjær K, Muri H, Kristjánsson JE, Boucher O, Schulz M, Cole JNS, Curry CL, Jones A, Haywood JM, Irvine PJ, Ji D, Moore JC, Karam DB, Kravitz B, Rasch PJ, Singh B, Yoon J-H, Niemeier U, Schmidt H, Robock A, Yang S, Watanabe S (2013) The hydrological impact of geoengineering in the Geoengineering Model Intercomparison Project (GeoMIP). *J Geophys Res: Atmos* 118(19):11036–11058
- Tingley MP, Stine AR, Huybers P (2014) Temperature reconstructions from tree-ring densities overestimate volcanic cooling. *Geophys Res Lett* 41:7838–7845
- Tjiputra JF, Grini A, Lee H (2016) Impact of idealized future stratospheric aerosol injection on the large-scale ocean and land carbon cycles. *J Geophys Res Biogeosci* 121(1):2–27
- Trisos CH, Amatulli G, Gurevitch J, Robock A, Xia L, Zambri B (2018) Potentially dangerous consequences for biodiversity of solar geoengineering implementation and termination. *Nature Ecology & Evolution* 2:475–482
- van Vuuren DP, Edmonds J, Kainuma M, Riahi K, Thomson A, Hibbard K, Hurtt GC, Kram T, Krey V, Lamarque J-F, Masui T, Meinshausen M, Nakicenovic N, Smith SJ, Rose SK (2011) The representative concentration pathways: an overview. *Clim Chang* 109:5–31
- Walther G-R, Post E, Convey P, Menzel A, Parmesan C, Beebee TJC, Fromentin J-M, Hoegh-Guldberg O, Bairlein F (2002) Ecological responses to recent climate change. *Nature* 416(6879):389–395
- Wolkovich EM, Cook BI, Allen JM, Crimmins TM, Betancourt JL, Travers SE, Pau S, Regetz J, Davies TJ, Kraft NJB, Ault TR, Bolmgren K, Mazer SJ, McCabe GJ, McGill BJ, Parmesan C, Salamin N, Schwartz MD, Cleland EE (2012) Warming experiments underpredict plant phenological responses to climate change. *Nature* 485(7399):494–497
- Xia L, Robock A, Tilmes S, Neely RRII (2016) Stratospheric sulfate geoengineering could enhance the terrestrial photosynthesis rate. *Atmos Chem Phys* 16(3):1479–1489